Spectrochimica Acta Part B: Atomic Spectroscopy 201 (2023) 106617

Contents lists available at ScienceDirect

Spectrochimica Acta Part B: Atomic Spectroscopy

journal homepage: www.elsevier.com/locate/sab

Comparison of light capturing approaches in Laser-Induced Breakdown Spectroscopy (LIBS) for multichannel spectrometers

María Gabriela Fernández-Manteca [a], Marina Martínez-Minchero [a,b], Asier García-Escárzaga [d,e], Alain A. Ocampo-Sosa [a,f], Jesús Mirapeix [a,b,c], José J. Valdiande [b], José Miguel López-Higuera [a,b,c], Luis Rodríguez-Cobo [a,b,c], Adolfo Cobo [a,b,c,*]

[a] Instituto de Investigación Sanitaria Valdecilla (IDIVAL), Santander, Spain
[b] Photonics Engineering Group, Universidad de Cantabria, Santander, Spain
[c] CIBER de Bioingeniería, Biomateriales y Nanomedicina (CIBER-BBN), Instituto de Salud Carlos III, Madrid, Spain
[d] Department of Prehistory, Institute of Environmental Science and Technology (ICTA-UAB), Universitat Autònoma de Barcelona, Bellaterra, Spain
[e] Department of Archaeology, Max Planck Institute for Geoanthropology, Jena, Germany
[f] Servicio de Microbiología, Hospital Universitario Marqués de Valdecilla, Santander, Spain

ARTICLE INFO

Keywords:
LIBS spectroscopy
Optical plasma emission
Multichannel spectrometer
Köhler optics

ABSTRACT

LIBS technique requires the spectroscopic analysis of the light emitted by a laser-induced plasma plume. One challenge of the different approaches to capture the plasma light emission is the significant shot-to-shot variations of the plume inhomogeneities, position, and morphology. This is even more challenging when multichannel CCD spectrometers are used, because the light should be homogeneously divided among multiple capturing optical fibers (typically up to 8 fibers) with stable spectral efficiency for all channels. Otherwise, any further analysis of the atomic emission spectra involving multiple channels, such as line intensity ratios, Boltzmann plots, or calibration-free LIBS, could be compromised by the morphology-dependent spectral artifacts induced by the collection optics. In this work, we assess the performance of several collection optics in terms of overall capturing efficiency and channel-to-channel variations due to changes in plasma morphology. Results clearly show that this could be an issue even with the approaches with the best spatial homogenization, including optical fibers and Köhler optics.

1. Introduction

Laser-Induced Breakdown Spectroscopy (LIBS) offers information on the composition of a sample at the atomic level by the spectral analysis of the optical emission of a plasma induced by a pulsed laser generated during the material ablation [1]. For typical samples, plasma has the shape of a plume, up to several millimeters in size, but with significant shot-to-shot variations of the plume position, morphology, and spatial inhomogeneities of electronic temperature and density [2,3]. This represents a challenge for the capturing optics that carries the optical emission to the spectrometer. The broad spectral range of interest, from the far ultraviolet (<200 nm) to the near-infrared (>900 nm), also affects the collection optics design. Common applications (such as quantitative analysis) try to perform a spatial integration of the light emitted by the plume while reducing chromatic aberrations so that shot-to-shot variations can be minimized.

Many optical solutions have been proposed in the literature [4]. A common approach involves a single or multiple lens arrangement that projects the plasma image over the slit of the spectrometer. With this solution, shape variations are translated and sampled at the slit plane. Besides, atomic emission lines for some elements are mainly located in the ultraviolet spectral range (<400 nm), so finding suitable achromatic lenses is difficult, and chromatic aberration could produce shot-to-shot spectral variations. An alternative is the use of a pierced parabolic mirror [8] that focuses the plasma emission onto the spectrometer without chromatic aberration and high efficiency due to the large area of the mirror. However, any imaging optical arrangement could suffer from variable collected light intensity due to plasma shape variations in each laser shot.

This problem could be mitigated by using an optical fiber at the image plane that integrates the captured light over their core area and numerical aperture [5] and, after guiding, produces a stable light

* Corresponding author at: Instituto de Investigación Sanitaria Valdecilla (IDIVAL), Santander, Spain.
E-mail address: adolfo.cobo@unican.es (A. Cobo).

https://doi.org/10.1016/j.sab.2023.106617
Received 16 November 2022; Received in revised form 9 January 2023; Accepted 10 January 2023
Available online 14 January 2023

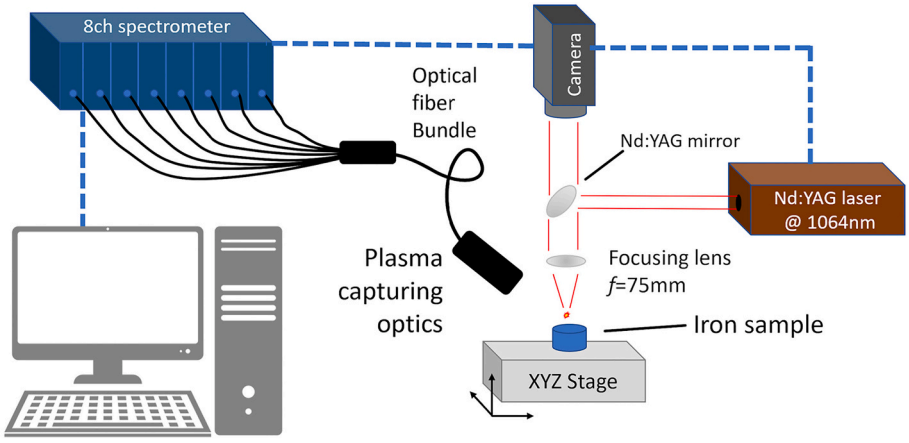

Fig. 1. LIBS experimental setup.

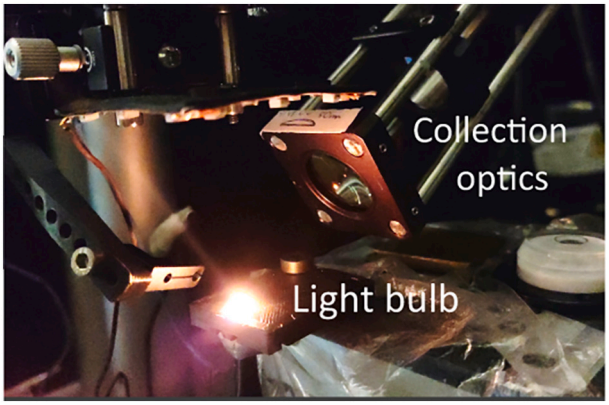

Fig. 2. Photograph of the experimental model of the plasma plume.

pattern over the spectrometer slit. Choosing different focal lengths of lenses, plasma images smaller or larger than the core size can reduce the intensity fluctuations. A more common arrangement in published experiments is the use of a bare multimode, high core diameter (up to 1 mm) optical fiber connected to the spectrometer, placed at several millimeters from the plasma. This produces a stable capturing efficiency, almost free from chromatic aberrations, and with sufficient capturing efficiency due to the proximity to the plasma plume [6].

However, the problem of shot-to-shot fluctuations is even more challenging when a multichannel CCD spectrometer is used, i.e., a set of multiple independent but synchronized CCD spectrometers in different spectral ranges, that require a fiber bundle to split the collected plasma emission among all of them. A non-comprehensive random survey of 50 LIBS experiments published in 2022 shows that 50% of them use this kind of instrument. Incidentally, all LIBS systems deployed or to be deployed in Mars rovers are based on multichannel spectrometers [7]. This widespread use can be attributed to their combination of broad spectral range, high resolution, high optical throughput, and low cost [9].

For multichannel spectrometers, plasma emission should be captured by a bundle of optical fibers (typically up to 8 fibers), and different channels analyze different spectral regions. Shot-to-shot spectral variations of the captured spectra are unavoidable in LIBS due to changes in plasma properties, but a homogenous, repeatable splitting of light intensity and spectral content among the channels is expected. Otherwise, any further analysis of the atomic emission spectra involving different channels, such as line intensity ratios, Boltzmann plots, or calibration-free LIBS, could be compromised by the morphology-dependent spectral artifacts induced by the collection optics. We understand by "spectral artifacts" the unwanted shot to shot amplitude variations in different spectral ranges of the captured spectrum that cannot be attributed to naturally occurring changes in plasma emission but to changes in the light splitting performed by the collection optics that affect the capturing efficiencies of each channel.

One proposed solution uses a fiber homogenizer, a short (typically about 5 cm in length) silica rod placed in front of the fiber bundle [10]. More complex arrangements have been proposed, particularly the use of the Köhler illumination principle. This arrangement of lenses is typically used in microscopes to obtain a diffuse illumination at the sample plane irrespective of the shape and light spatial distribution of the light source [11]. In the case of LIBS capturing optics, a Köhler configuration can project the plasma emission on a homogenous spot at the object plane, thus significantly reducing shot-to-shot fluctuations. A LIBS-specific design was proposed recently by Lucchi et al. [12]. It is based on two plano-convex lenses, and achieves an excellent homogenization performance. However, it has the drawback of a large spot at the object plane (~4 mm size) that results in poor collection efficiency at the optical fiber plane for typical fiber core diameters. An improved design with high homogenization and a smaller spot (i.e., <1 mm diameter) would need more lenses and typically larger working distances for the optics. Besides, attaining good performance over the required wide spectral range is always challenging.

In this work, we assess the performance of several collection optics in terms of overall capturing efficiency and channel-to-channel variations due to changes in the shot-to-shot plasma morphology for a widely used LIBS setup involving a multichannel (8 channels) spectrometer.

2. Materials and methods

2.1. Experimental setup

Experiments were performed with the LIBS setup shown in Fig. 1.

We used a Q-switched Nd:YAG laser (Lotis LS-2134D-MH) emitting 12 ns pulses at 1064 nm with a 10 Hz repetition rate. The laser beam was focused on the sample with a fused silica lens of 75 mm focal length. The sample could be moved in three axes with a motorized stage, and the sample's surface was observed with a coaxial RGB camera. The optical emission of the plasma was captured by the different optics used in this study and sent to an 8-channel CCD-based spectrometer [10] ULS2048-USB2-RM) with a total spectral range from 178 to 889 nm, and variable resolution between 0.015 and 0.06 nm. An 8-fiber bundle with fused silica multimode optical fibers of 200 μm core diameter and 220 μm cladding diameter was used to split the incoming light to the different channels. The fibers of the bundle are arranged in a circular pattern with a total diameter of 800 μm.

To verify the influence of plasma morphology variations, we

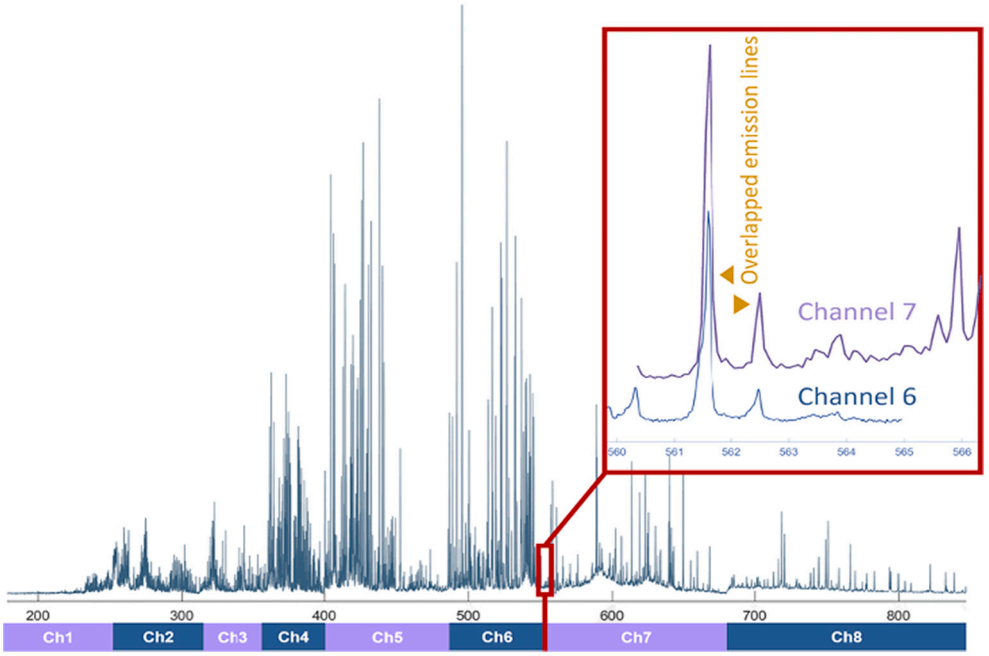

Fig. 3. Example of Iron LIBS spectrum. The inset shows the spectral range overlapped in two adjacent channels. Amplitude difference can be attributed to the different gratings and blaze wavelength sin each channel.

designed an experimental model of the plasma plume. It is based on a small (4 mm height by 3 mm wide) incandescent light bulb covered by a Polytetrafluoroethylene (PTFE) diffuser. This lamp has a wide spectral range of emission and size slightly larger than a typical plasma plume. It was placed on an XYZ automatic positioner, and its position was scanned within a 2x2x2mm cube to simulate shot-to-shot changes in the plasma plume. Fig. 2 shows a photograph of the experimental model.

For each position, the overall capturing efficiency was derived from the wavelength integration of channels 4–7 (360–680 nm), while the homogenization performance was estimated from the mean intensity ratio at three overlapped wavelength ranges: 399–401 nm between channels 4&5, 489–492 nm (channels 5&6), and 561–564 nm (channels 6&7). Best arrangements correspond to those with higher collection efficiency and more stable intensity ratios at channel edges, that is, less dependence of the intensity ratio on the shift in position.

Additionally, LIBS experiments were performed on an ingot of pure Iron obtained in a levitation induction furnace to assure >99.99% purity. Iron was chosen due to the high number of emission lines and single element composition. The ingot was cut flat and polished to further assure sample homogeneity. To verify if the light reaching different channels changes on a shot-to-shot basis, we rely on the fact that a spectral range of a few nanometers is duplicated in adjacent channels of the spectrometer. This overlap allows us to monitor changes in the collected intensity for the same wavelengths in different channels, a situation that should not occur in the case of an ideal collection optics. To perform these experiments, the plasma emission from a burst of 100 laser shots (30 mJ pulse energy) at five spatial points of the sample's surface were collected with the 8-channel spectrometer, using 1 μs gate delay and 1 ms acquisition time. The crater size was 200 μm in diameter, resulting in an irradiance of 8 GW/cm^2. First 5 spectra in each spatial point were discarded as cleaning shots. Those conditions are representative of a typical LIBS experiment.

Fig. 3 shows an example of the captured spectrum from the Iron sample. The inset depicts the Fe I emission lines at 561.56 and 562.45 nm, captured in both channels 6 and 7. Other Fe I emission lines in the overlapped range were identified and measured: 399.74 nm and 400.52 nm in channels 4&5, and 490.33 nm in channels 5&6. Tracking the intensities ratio of the same emission line in adjacent channels indicates undesirable shot-to-shot channel splitting variations.

2.2. Collection optics

Several designs of collection optics have been tested. All of them have been added to the optical fiber bundle that splits the light to the eight channels of the spectrometer (the fiber bundle comprises eight fibers of 200 μm core diameter each one), and placed at an angle of about 45° with respect to the horizontal. The tested optical arrangements are the following (See Fig. 5):

1. Nothing added: the 8-fiber bundle is placed close to the plasma plume (10 mm distance) and aligned for maximum captured light intensity.
2. A multimode, 1-m length, 1 mm core diameter homogenizing fiber is connected to the fiber bundle, and one extreme is placed close to the plasma plume (10 mm distance). In this case, the overall diameter of the 1 mm fiber is slightly larger than the fiber bundle diameter (800 μm), so most of the captured light is uniformly projected on the eight cores of the fiber bundle. The numerical aperture is the same for the optical fiber and the fiber bundle (NA = 0.22).
3. An aspheric UV-enhanced collimator (model 74-UV, Ocean Insight) is placed before the 1 mm diameter homogenizing fiber and aligned to the plasma plume.
4. The same aspheric UV-enhanced collimator is directly connected to the fiber bundle without the homogenizing fiber.
5. A commonly used arrangement of two plano-convex lenses with 50 and 40 mm focal lengths, respectively, is aligned with the plasma plume at the focal distance of the first lens (50 mm), and the plasma plume is imaged onto the 1 mm homogenizing fiber with magnification M = 0.85. Due to the expected size of the plasma, its image on the surface of the optical fiber is of the order of the fiber core.
6. The same optical arrangement of two lenses (50 mm + 40 mm) is used directly with the fiber bundle, without the 1 mm homogenizing fiber.

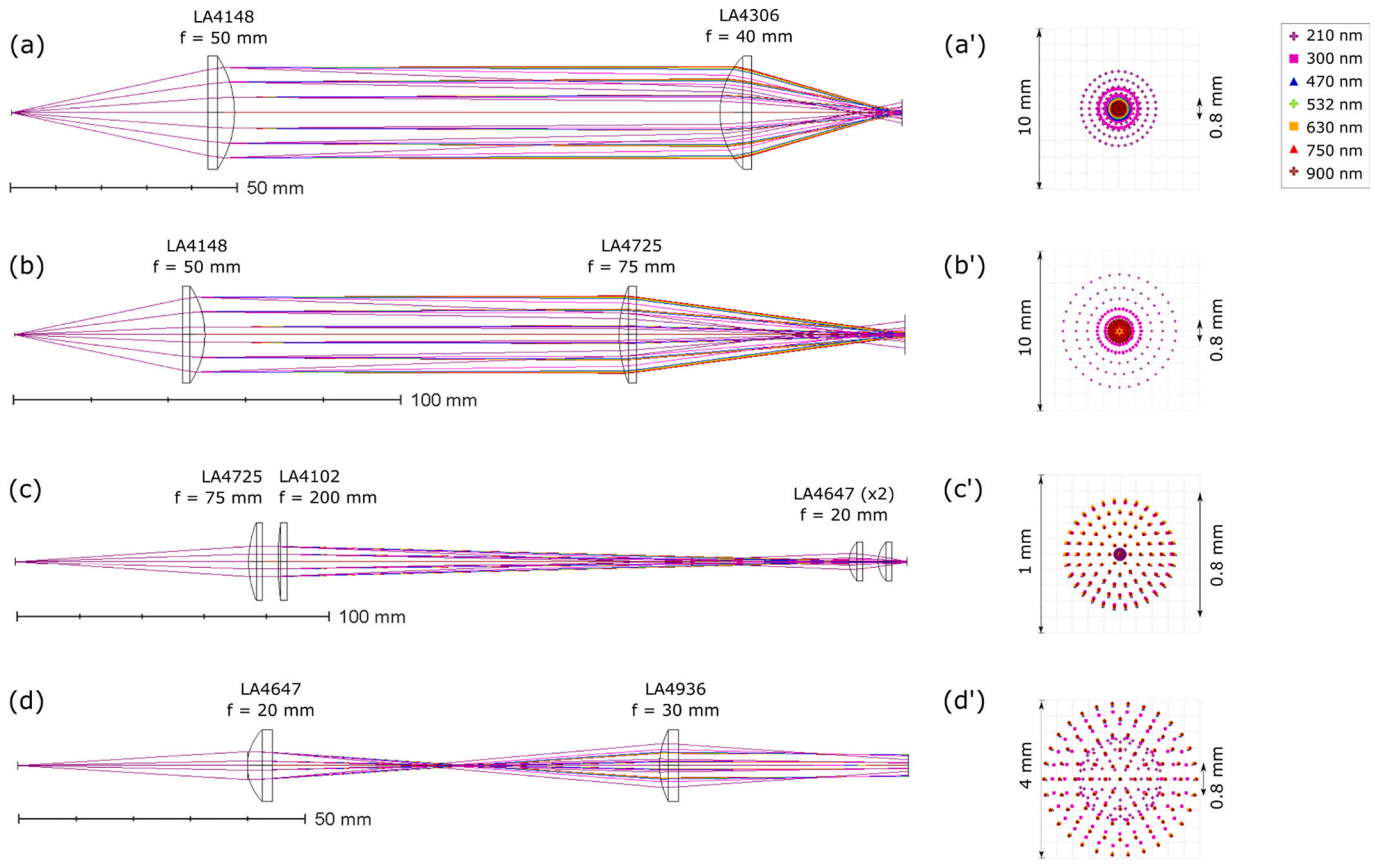

Fig. 4. Four Köhler designs optimized for collection efficiency, homogenization, and spectral range of operation.

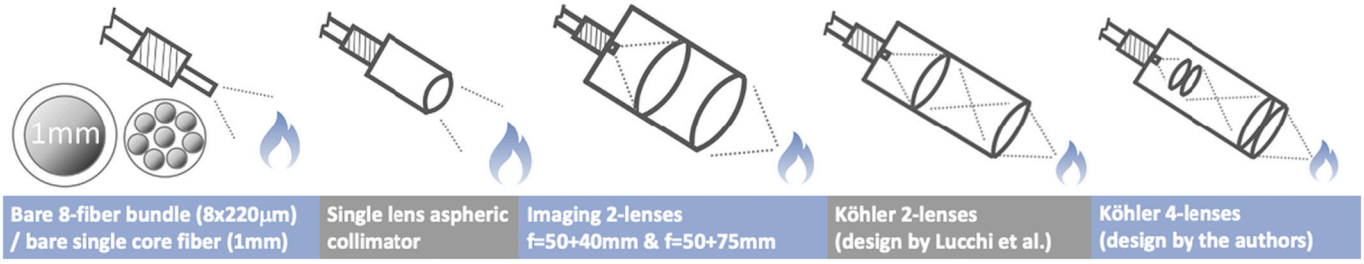

Fig. 5. Summary of the tested optical arrangements for capturing the plasma emission.

Table 1
UV fused silica plano-convex lenses used in the optical arrangements #5-#12 to capture the plasma emission [13]. *Design wavelength is 588 nm for all lenses.

Reference	Focal Length (mm)*	Diameter (inches)	Radius of Curvature (mm)	Center Thickness (mm)	Edge Thickness (mm)
LA4148	50.2	1″	23.0	5.8	2.0
LA4306	40.1	1″	18.4	7.1	2.0
LA4725	75.3	1”	34.5	4.4	2.0
LA4102	200.7	1”	92.0	2.9	2.0
LA4647	20.1	1/2”	9.2	4.3	1.8
LA4936	30.1	1/2”	13.8	3.4	1.8

7. An arrangement of two plano-convex lenses with 50 and 75 mm focal lengths is aligned with the plasma plume at the focal distance of the first lens (50 mm), and the plasma plume is imaged onto the 1 mm homogenizing fiber with magnification M = 1.5. In this case, the size of the plasma plume image larger than the

Table 2
Comparison of the overall (spectrally integrated) capturing efficiency of the different optical setups (relative to the one with the highest performance).

Collection optics	Capturing efficiency
Only 8-fiber bundle	80.9%
1 mm fiber	76.1%
Aspheric collimator +1 mm fiber	67.1%
Aspheric collimator	78.8%
Imaging 2 lenses 50 + 40 mm + 1 mm fiber	75.7%
Imaging 2 lenses 50 + 40 mm	82.5%
Imaging 2 lenses 50 + 75 mm + 1 mm fiber	88.0%
Imaging 2 lenses 50 + 75 mm	**100.0%**
Köhler 4 lenses +1 mm fiber	46.4%
Köhler 4 lenses	51.7%
Köhler 2 lenses +1 mm fiber	73.5%
Köhler 2 lenses	77.2%

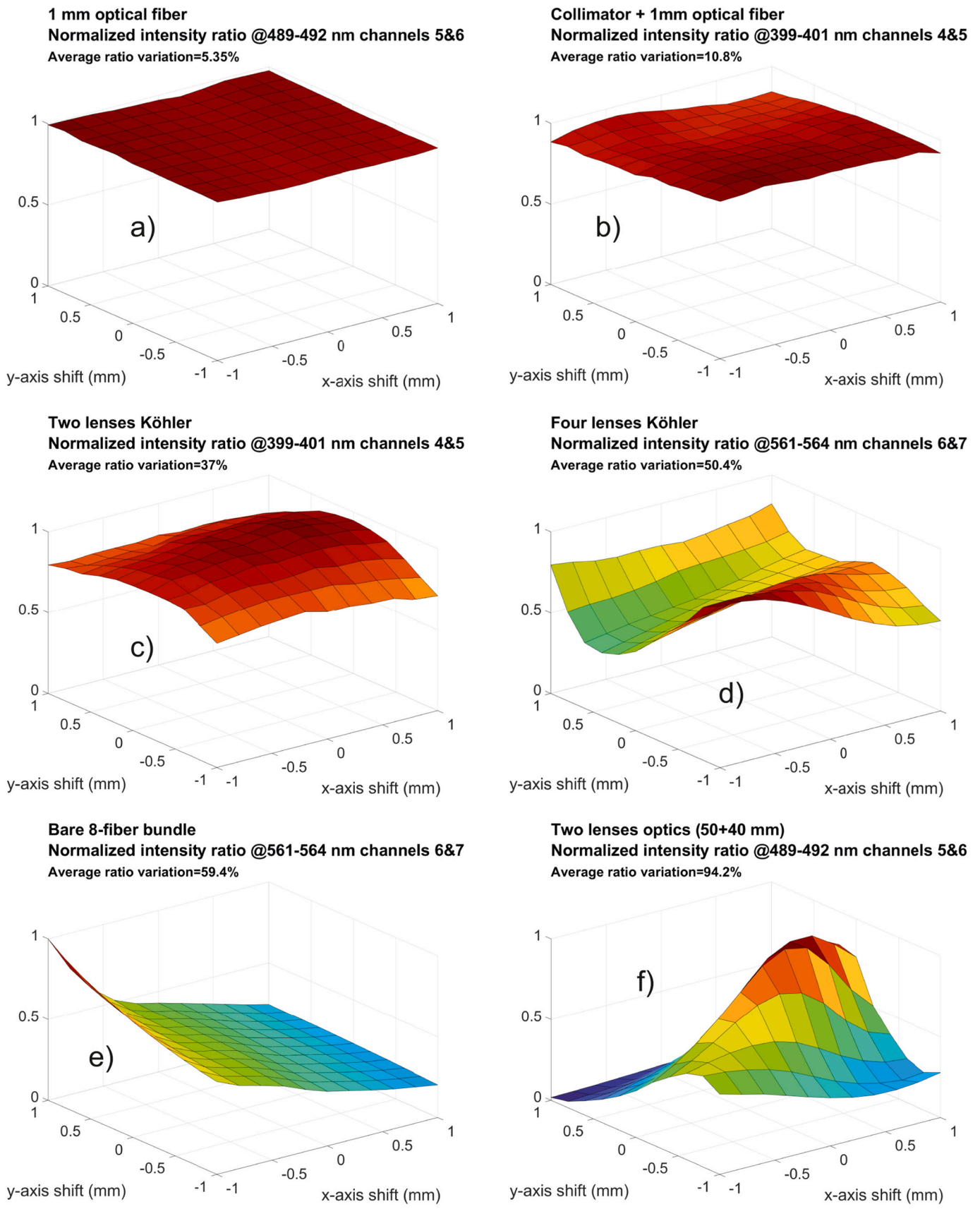

Fig. 6. Measurement of the light intensity ratio in overlapped spectral windows for different optical arrangements. The vertical axis is the normalized ratio. Average is performed for the three spectra channel edges. Only a representative selection of measurements is shown: a) 1 mm optical fiber, b) Collimator added, c) Two-lenses Köhler design; d) Four-lenses Köhler design, e) Bare 8-fiber bundle, f) Two-lenses (50 + 40 mm focal lengths).

Table 3
Comparison of the homogenization performance of the different optical approaches with a single figure of merit calculated as the maximum variation of the light intensity ratio averaged at the three overlapped spectral windows. The lower the ratio variation, the better.

Collection optics	Avg. ratio variation
Only 8-fiber bundle	59.4%
1 mm fiber	**5.3%**
Aspheric collimator +1 mm fiber	10.8%
Aspheric collimator	34.4%
Imaging 2 lenses 50 + 40 mm + 1 mm fiber	41.1%
Imaging 2 lenses 50 + 40 mm	94.2%
Imaging 2 lenses 50 + 75 mm + 1 mm fiber	26.5%
Imaging 2 lenses 50 + 75 mm	94.7%
Köhler 4 lenses +1 mm fiber	23.7%
Köhler 4 lenses	37.0%
Köhler 2 lenses +1 mm fiber	19.0%
Köhler 2 lenses	50.4%

core of the capturing fiber, so only a portion of the plasma area is sampled.

8. The same optical arrangement of two lenses (50 mm + 75 mm) is placed directly before the fiber bundle, without the 1 mm homogenizing fiber.
9. A Köhler design with two lenses proposed by Lucchi et al. [12], placed before the 1 mm fiber. It is a simpler design but with lower capturing efficiency.
10. The same Köhler design of two lenses, but directly connected to the fiber bundle.
11. A Köhler design based on four lenses is placed before the 1 mm homogenizing fiber. The design is shown in Fig. 4, and details are given in the following paragraphs.
12. The same Köhler design of 4 lenses, but directly connected to the fiber bundle.

Collection optics #11 in the previous list is a new Köhler design proposed in this work that tries to optimize the collection efficiency, homogenization, and spectral range. Several designs were analyzed using Zemax's OpticStudio® to assess their performance for this application; they are shown in Fig. 4.

The first two designs - (a) and (b) in Fig. 4 - use two lenses and achieve a good homogenization and a small spot size (slightly over the 800 μm diameter target to illuminate the 8-fiber bundle fully), for a spectral range from 300 to 900 nm. However, smaller wavelengths are spread over a larger area, as seen in the simulated spot diagrams for the 200 nm wavelength in Fig. 4 (a)' and (b)'. This behavior can be explained by the sharp refractive index increment of fused silica in the UV region [13]. An improved performance was found with the four lenses design shown in Fig. 4 (c), achieving a maximum spot size of 800 μm for the entire wavelength range from 200 to 900 nm. This is the Köhler design #11 implemented for the experiments. The other Köhler design - Fig. 4 (d) - corresponds to the one proposed by Lucchi et al. It has excellent spectral and spatial homogenization, but with a spot size of 4 mm, thus resulting in poor collection efficiency with typical optical fiber sizes. Table 1 shows the details of the lenses chosen for the designs.

For each optical arrangement, an experiment with the model of the plasma plume and a LIBS experiment on an Iron sample were performed. In the next section, we show the results concerning the overall light-capturing efficiency of each one and, most importantly, their performance in terms of the shot-to-shot variations of the channel splitting of light and its impact on the LIBS spectrum analysis.

3. Results and discussion

3.1. Overall light capturing efficiency

Different approaches for light capturing result in different optical efficiency and, therefore, affect the signal-to-noise ratio of emission lines and any subsequent qualitative or quantitative analysis. We used the experimental model of the plasma plume (small light bulb) to compare the capturing efficiency of the different optical configurations. Collection efficiency was estimated from the spectral integration of channels 4 to 7 (360 to 680 nm), as most of the spectral content of the incandescent bulb is concentrated in that range. Table 2 shows a summary of the results. The spectral efficiency is shown relative to the best-performing configuration, which is the two-lenses optics with 50 and 75 mm focal lengths. This result was expected due to the large size of the first lens (1″ diameter) and the low numerical aperture (NA = 0.19). The configuration with the lowest performance is the 2-lenses Köhler design, with a relative efficiency of approximately 50%. Interestingly, the bare optical fiber of 1 mm core diameter placed at 10 mm from the plasma plume reached a 76% relative efficiency. Nevertheless, there is only a two-fold difference between the worst and best performing arrangement, which should have a minor impact in a typical LIBS experiments.

3.2. Shot-to-shot variations in the captured light

To estimate the ability of each optical configuration to reduce the shot-to-shot variations, we have measured the light intensity detected in the overlapped spectral ranges of different channels and its variation due to plasma movements. The experimental model of the plasma plume (small light bulb) was placed at different points within a cube of 2x2x2mm. At each spatial point, the light intensity was calculated by integrating the signal at the following overlapped spectral windows: 399–401 nm for channels 4 and 5; 489–492 nm for channels 5 and 6; and 561–564 nm for channels 6 and 7. For ideal capturing optics, the ratio of light intensity of two channels at the same spectral window should remain constant irrespective of the plasma position if a perfect homogenization of the light over the 8-fiber bundle is expected. Any change in the light intensity ratio in those measurements will translate to spectral artifacts in the captured spectrum in LIBS experiments with real plasma plumes.

Fig. 6 shows a selection of the light intensity ratio measurements for representative cases, including the best and worst-performing optics. The vertical axis shows the normalized light intensity ratio at the indicated spectral window and channels. Only the horizontal spatial scanning of ±2 mm of the model of the plasma plume was considered.

It can be seen from Fig. 6 that the best-performing optics is the 1 mm core-diameter optical fiber, with a maximum variation of the light intensity ratio of about 5% (averaged in the three overlapped spectral windows at the channel edges). In contrast, other configurations, such as the two-lenses arrangement, show much more variations, close to 100%. Adding a collimator to the optical fiber results in higher variations (lower homogenization), while the Köhler designs do not provide a better homogenization as expected.

To get an overall ranking of the performance of the different approaches, for each one, the maximum variation of the light intensity ratio was calculated at the three spectral windows, and the results were averaged to get a single figure of merit. The results are shown in Table 3.

From Table 3, it can be seen that the best approach is the use of the bare 1 mm optical fiber connected to the 8-fiber bundle. As expected, adding this homogenizing fiber improves the metrics for all configurations. However, the two lenses arrangement, widely used in reported LIBS experiments, results in very poor performance if no homogenizing fiber is used. Additionally, Köhler designs do not improve homogenization over using an optical fiber as capturing element. Most interestingly, the best-performing approach still has a 5.3% mean variation of the light intensity ratio at the same spectral window in adjacent channels, meaning that the effect of variable light splitting is not negligible and should be considered in the analysis of the LIBS spectral data.

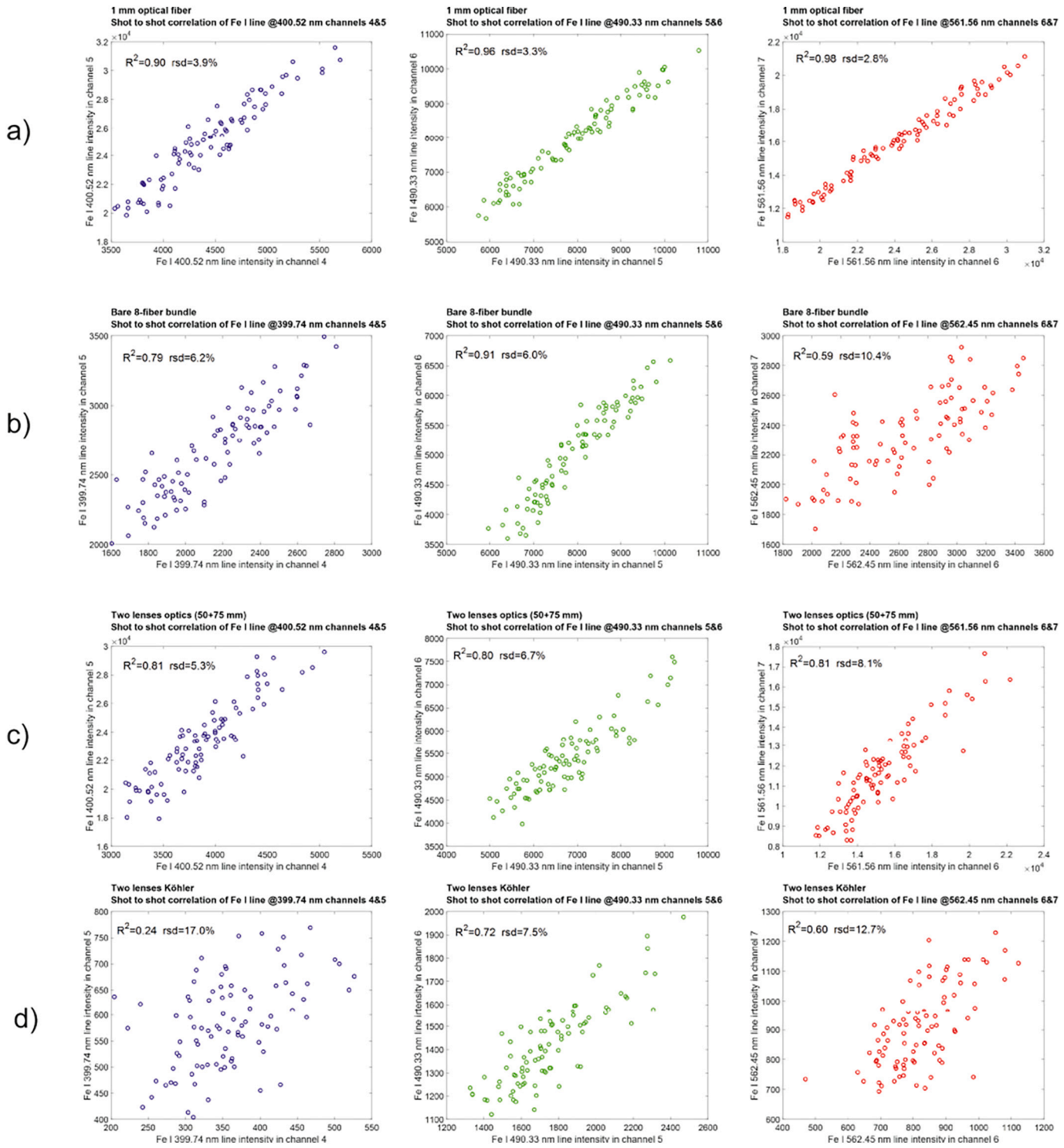

Fig. 7. Correlation between the intensities of the same emission line of Fe I when measured by two adjacent channels in the overlapped spectral ranges. Only the results for four of the configurations are included (including the one with the best and worst performance). In each row, three charts corresponding to one emission line in each spectral range are shown, from top to bottom: a) 1 mm optical fiber, b) bare 8-fiber bundle, c) two-lenses arrangement (50 + 75 mm focal lengths) and d) two-lenses Köhler design.

3.3. Impact on LIBS experiments

To assess the impact of shot-to-shot plasma plume variations in the inter-channel distribution of light in LIBS experiments, we have performed ablation experiments with the above-described setup on a sample of pure Iron. For each design of collection optics, we calculated the intensity of the same emission line of Fe I at 399.74, 400.52, 490.33 nm, 561.56, and 562.45 nm collected in the overlapped spectral ranges. Fig. 7 shows a representative set of the results from all the tested collection optics. In each chart, the intensity of the same line, measured in two different channels, is plotted for all the laser shots, and the correlation coefficient R^2 is calculated. For ideal capturing optics with no spectral artifacts, a value of 1 is expected. It can be seen that, again, the use of a bare fiber optic before the 8-fiber bundle gives the best

Table 4
Performance of all the tested collection optics in terms of inter-channel variations of the emission lines in LIBS experiments.

Collection optics	Avg. R^2 coeff.	Avg. RSD
Only 8-fiber bundle	0.74	7.2%
1 mm fiber	**0.92**	4.1%
Aspheric collimator +1 mm fiber	0.74	4.9%
Aspheric collimator	0.83	4.0%
Imaging 2 lenses 50 + 40 mm + 1 mm fiber	0.77	5.7%
Imaging 2 lenses 50 + 40 mm	0.74	7.2%
Imaging 2 lenses 50 + 75 mm + 1 mm fiber	0.91	**3.9%**
Imaging 2 lenses 50 + 75 mm	0.76	7.1%
Köhler 4 lenses +1 mm fiber	0.89	4.3%
Köhler 4 lenses	0.59	7.2%
Köhler 2 lenses +1 mm fiber	0.81	6.6%
Köhler 2 lenses	0.52	10.3%

homogenization, with R^2 values close to 1 in all the three overlapped spectral ranges (first row of Fig. 7). In contrast, the two-lenses Köhler design has the lowest R^2 values (last row of Fig. 7). It is clear from the figures that shot-to-shot ratios of the selected emission lines suffer a significant variability that only can be attributed to an unwanted variable light splitting between the channels.

A summary of the performance for all the tested collection optics is shown in Table 4. In this table, the correlation coefficients (as shown in Fig. 7) have been averaged for the five emission lines at the three different spectral ranges. Additionally, the relative standard deviation (RSD) of the ratio of the emission lines has been calculated for the 100 laser shots and averaged for the five emission lines. It can be seen that two designs give the best results: single 1 mm optical fiber (#2) and the same fiber with added imaging lenses (#7), in both cases with an averaged R^2 coefficient of 0.9 and averaged RSD of 4%. The additional lenses also improve the collection efficiency. Removing the homogenizing fiber greatly increases variability in all cases.

These results show that, even for one of the best homogenization approaches to prevent shot-to-shot inter-channel variations, some small and non-negligible spectral artifacts are still present, and this should be taken into account in any further spectral processing, for example, for any quantitative LIBS analysis involving emission lines in different channels.

4. Conclusions

We have analyzed different designs of collection optics typically used by the LIBS research community to study their performance when used with multichannel spectrometers routinely employed to increase LIBS experiments' spectral range and resolution.

The tested configuration of collection optics involves several optical arrangements placed before the fiber bundle used by this kind of spectrometer: homogenizing single-core optical fiber, two lens systems with different focal lengths, and two Köhler designs with improved homogenization capabilities.

To assess the homogenization performance of each setup, we leverage the overlapped spectral range in several adjacent channels of the spectrometer. As they measured the same wavelengths, any shot-to-shot variation could be attributed to homogenization issues.

Our results show that even for one of the best homogenization approaches to prevent shot-to-shot inter-channel variations (namely, a long single-core optical fiber without any additional lenses), some small but non-negligible spectral artifacts are still present, and this should be taken into account in any further spectral processing, for example, for any quantitative LIBS analysis involving emission lines in different channels.

Declaration of Competing Interest

The authors declare that they have no known competing financial interests or personal relationships that could have appeared to influence the work reported in this paper.

Data availability

Data will be made available on request.

Acknowledgments

This work was supported by the R + D project PID2019-107270RB-C21 (funded by MCIN/ AEI /10.13039/501100011033) and by Plan Nacional de I + D + and Instituto de Salud Carlos III (ISCIII), Subdirección General de Redes y Centros de Investigación Cooperativa, Ministerio de Ciencia, Innovación y Universidades, Spanish Network for Research in Infectious Diseases (REIPI RD16/0016/0007), CIBERINFEC (CB21/13/00068), CIBER-BBN (BBNGC1601), cofinanced by European Development Regional Fund "A way to achieve Europe". A. O.-S was financially supported by the Miguel Servet II program (ISCIII-CPII17–00011). AGE was supported by the Catalonia Government throughout a Beatriu de Pinós fellowship (grant number 2020 BP 00240). We thanks Dr. A. Picón for providing the pure iron ingot and helpful suggestions to improve the experimental setup.

References

[1] L. Radziemski, D. Cremers, A brief history of laser-induced breakdown spectroscopy: from the concept of atoms to LIBS 2012, Spectrochim. Acta B At. Spectrosc. 87 (2013) 3–10.
[2] C. Aragón, J.A. Aguilera, Characterization of laser induced plasmas by optical emission spectroscopy: a review of experiments and methods, Spectrochim. Acta B At. Spectrosc. 63 (9) (2008) 893–916.
[3] Y. Fu, Z. Hou, T. Li, Z. Li, Z. Wang, Investigation of intrinsic origins of the signal uncertainty for laser-induced breakdown spectroscopy, Spectrochim. Acta B At. Spectrosc. 155 (2019) 67–78.
[4] T. Li, S. Sheta, Z. Hou, J. Dong, Z. Wang, Impacts of a collection system on laser-induced breakdown spectroscopy signal detection, Appl. Opt. 57 (21) (2018) 6120–6127.
[5] S.V. Shabanov, I.B. Gornushkin, J.B. Winefordner, Radiation from asymmetric laser-induced plasmas collected by a lens or optical fiber, Appl. Opt. 47 (11) (2008) 1745–1756.
[6] R. Noll, Laser-Induced Breakdown Spectroscopy: Fundamentals and Applications, Springer, 2012.
[7] R.C. Wiens, X. Wan, J. Lasue, S. Maurice, Laser-induced breakdown spectroscopy in planetary science, in: Laser-Induced Breakdown Spectroscopy, Elsevier, 2020, pp. 441–471.
[8] D. Redoglio, U. Perini, S. Musazzi, LIBS collection optics: Comparative analysis of different mirror-based configurations, in: In 2014 Fotonica AEIT Italian Conference on Photonics Technologies, IEEE, 2014, May, pp. 1–4.
[9] J.E. Carranza, E. Gibb, B.W. Smith, D.W. Hahn, J.D. Winefordner, Comparison of nonintensified and intensified CCD detectors for laser-induced breakdown spectroscopy, Appl. Opt. 42 (30) (2003) 6016–6021.
[10] https://www.avantes.com/products/fiber-optics/fiber-optic-homogenizer/. Accessed 14 November 2022.
[11] R. Fischer, B. Tadic-Galeb, P. Yoder, Optical System Design, McGraw-Hill Education, 2008.
[12] J. Lucchi, M. Martinez, M. Baudelet, Homogenization of plasma emission collection for multichannel spectrometers, Appl. Spectrosc. 73 (10) (2019) 1228–1236.
[13] "UV Fused Silica Plano-Convex Lenses, Uncoated." Thorlabs, https://www.thorlabs.com/newgrouppage9.cfm?objectgroup_id=123. Accessed 14 November 2022.